Ab initio calculations of elastic properties of compressed Pt

E. Menéndez-Proupin[1] and Anil K. Singh[2]

[1]*Departamento de Física, Facultad de Ciencias, Universidad de Chile, Casilla 653, Santiago, Chile*
[2]*Materials Science Division, National Aerospace Laboratories, Bangalore 560 017, India*

First-principles calculations of the equation of state and single-crystal elastic constants of platinum have been carried out to 650 GPa using density-functional theory (DFT). The present equation of state deduced at 300 K agrees very well with the earlier computational results. The zero-pressure bulk modulus and its pressure derivative obtained in this study are in better agreement with the measured values than those from the earlier calculations. A comparison of the electronic energies indicates that the face-centered-cubic phase is more stable than the hexagonal-close-packed and body-centered-cubic phases up to at least 650 GPa. The values of the zero-pressure single-crystal elastic constants are also close to the experimental values. We also present the high-pressure electronic and vibrational densities of states, as well as the thermal contributions to the free energy.

I. INTRODUCTION

Despite its low compressibility, elemental platinum has been used extensively as a pressure standard in high-pressure x-ray diffraction experiments with diamond anvil cells, mainly because of high scattering power for x rays, stability of the ambient-pressure face-centered-cubic (fcc) phase to high pressures, and chemical inertness.[1–4] Further, its ability to absorb infrared radiation makes it an ideal absorber in laser-heated experiments. The equation of state (EOS) of platinum to 660 GPa based on experimental data from a two-stage light gas gun combined with a first-principles theoretical treatment has been used for the pressure estimation.[5] These data are in good agreement with the 300-K isotherm derived from the shock Hugoniot obtained in an earlier measurement.[6] The thermal EOS of platinum has been investigated more recently from first-principles calculations using the full-potential linear muffin-tin orbital density-functional theory (DFT) method combined with a pair-potential-based-mean-field approximation to the thermal free energy.[7] Although the EOSs proposed by different investigators agree well, the reliability of the platinum pressure scale has been questioned by Stacey and Davis.[8]

The parameter "pressure" in a first-principles calculation of the EOS refers to hydrostatic pressure. The stress states of the sample and pressure standard tend to deviate from hydrostatic as the pressure in the x-ray diffraction experiments is increased and ultimately become nonhydrostatic when stresses reach the 100-Gpa range. The modeling of the nonhydrostatic stress state and the resulting lattice strains permit interpretation of the diffraction data and extraction of the parameters corresponding to the hydrostatic stress state.[9–13] However, the single-crystal elastic constants as a function of pressure are required for the interpretation of the diffraction data obtained under nonhydrostatic condition with the conventional diffraction geometry.[13] The high-pressure elasticity data are usually obtained using the experimental values of the ambient-pressure elastic constants and their pressure derivatives in the Birch extrapolation formula.[14] Experimental studies of the elasticity of platinum are limited to measure-ments of the three single-crystal elastic constants at ambient pressure[16,15] and the pressure derivative of only C_{44}.[17] An x-ray diffraction study of platinum under nonhydrostatic compression deals with strength and rheological behavior.[18] Without complete information on the pressure derivatives of all the elastic constants, the role of platinum as a standard for precise pressure measurements will remain restricted.

In this paper, we employ a pseudopotential implementation of density-functional theory[19] to investigate the relative stabilities of the hexagonal-close-packed (hcp) and the body-centered-cubic (bcc) structures relative to the fcc structure of platinum to over 650 GPa, by comparing the unit cell electronic energy as a function of the volume. The EOS computed in this study is compared with those obtained in earlier calculations. In addition, we generate a complete set of single-crystal elastic constants as a function of volume (pressure) by subjecting the unit cell to suitable deformations and computing the corresponding stress tensors.

II. COMPUTATIONAL DETAILS

A. General

Standard DFT calculations provide the total energy $E_0(V)$ considering the atomic nuclei at rest. The analysis of E_0 allows us to calculate structural and elastic properties accurately at low and ambient temperature. This scheme is naturally improved by considering the free energy at finite temperature,

$$F(V,T) = E_0(V) + F_{phon}(V,T) + F_{elec}(V,T), \quad (1)$$

where the thermal correction to the electronic energy is given by

$$F_{elec}(V,T) = -\frac{\pi^2}{6}(k_B T)^2 D(E_F), \quad (2)$$

k_B being the Boltzmann constant and $D(E_F)$ the density of states (DOS) at the Fermi level. The phonon contribution can be obtained in the quasiharmonic approximation as

$$F_{phon}(V,T) = \int_0^{\omega_{max}} d\omega \, g(\omega)\left(\frac{\hbar\omega}{2} + k_B T \ln(1 - e^{-\hbar\omega/k_B T})\right),$$
(3)

where $g(\omega)$ is the phonon DOS. The term $\hbar\omega/2$ in the above equation gives the zero-point energy of the lattice vibration, and the second term gives thermal corrections. The pressure can be obtained by numerical differentiation of the free energy,

$$P = -\frac{\partial F}{\partial V} = P_0 + \Delta P,$$
(4)

where

$$P_0 = -\frac{\partial E_0}{\partial V}$$
(5)

and

$$\Delta P = -\frac{\partial F_{elec}}{\partial V} - \frac{\partial F_{phon}}{\partial V}.$$
(6)

The electronic energy $E_0 + F_{elec}$ has been calculated in the local density approximation (LDA) of DFT as implemented in the PWSCF code of the package QUANTUM ESPRESSO.[19] We have used a cutoff of 35 Ry for the plane wave expansion of the wave functions and 420 Ry for the charge density. To obtain a smooth DOS, the first Brillouin zone was sampled with a Monkhorst-Pack k mesh centered at the Γ point. The dimension of the k mesh was $25 \times 25 \times 25$ for the fcc and bcc structures, and $25 \times 25 \times 15$ for hcp. Unphysical oscillations of the DOS due to the discreteness of the k space grid have been eliminated using the first-order Methfessel-Paxton scheme[20] with a smearing parameter of 0.02 Ry. The stress tensor in QUANTUM ESPRESSO codes is calculated based on the expressions derived in Ref. 21. In the present calculation, only the electrons from the atomic shells $5d$, $6s$, and $6p$ are considered explicitly. The effect of the core electrons of Pt is included in an ultrasoft Rappe-Rabe-Kaxiras-Joannopoulos pseudopotential[22,23] available at the QUANTUM ESPRESSO web site. This pseudopotential includes scalar relativistic effect in the core electrons. We performed a few tests to establish the accuracy of our calculations, (1) using a norm-conserving pseudopotential, and (2) with full relativistic calculations with an ultrasoft pseudopotential, and found no significant changes in the EOS of fcc Pt.

The phonons and the thermal contribution to the free energy have been calculated in the quasi harmonic approximation using the PHONON code of QUANTUM ESPRESSO. The dynamical matrix was calculated in a $4 \times 4 \times 4$ mesh of the first Brillouin zone and interpolated to obtain a smooth phonon DOS and vibrational free energy. For the self-consistent electronic calculations involved in the computation of the dynamical matrix, we employed a reduced k mesh of $15 \times 15 \times 15$.

B. Energy and EOS

Figure 1 shows the electronic energy of the hcp and bcc
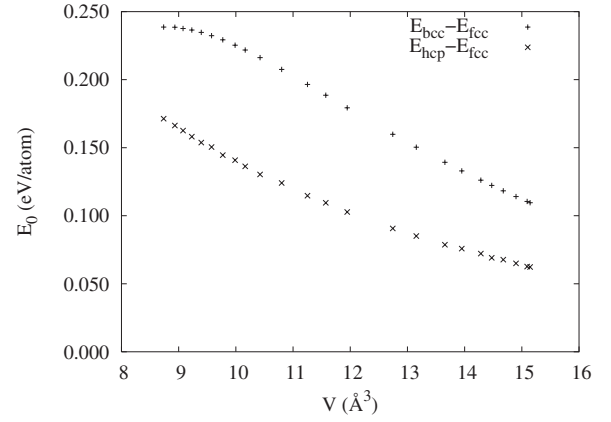
FIG. 1. Energies per atom of the hcp and bcc phases relative to the fcc energy. The Birch-Murnaghan energy is used.

phases relative to the stable fcc phase. For all pressures between 0 and 650 GPa, the energy difference is positive and the fcc is the stable phase. The hcp phase comes next in energy, and finally the bcc phase. Figure 2 shows the LDA electronic energy and the free energy at 300 K of the stable fcc phase of Pt. The full and dashed lines are fitted to these data using the following equation derived from the Vinet EOS:[24]

$$F(V) = F_0 + \frac{9V_0 B_0}{\eta^2}\{1 - e^{\eta(1-X)}[1 - \eta(1 - X)]\},$$
(7)

with

$$\eta = \frac{3}{2}(B_0' - 1), \quad X = \left(\frac{V}{V_0}\right)^{1/3},$$
(8)

where V_0 is the the equilibrium unit cell volume, B_0 is the bulk modulus, and B_0' is its pressure derivative. The parameters of the fitted curves are listed in Table I. There is a small dependence of the fitting parameters on the range of volume (or pressure) considered. For small pressures, the equilibrium volume tends to be smaller and the bulk modulus larger. The
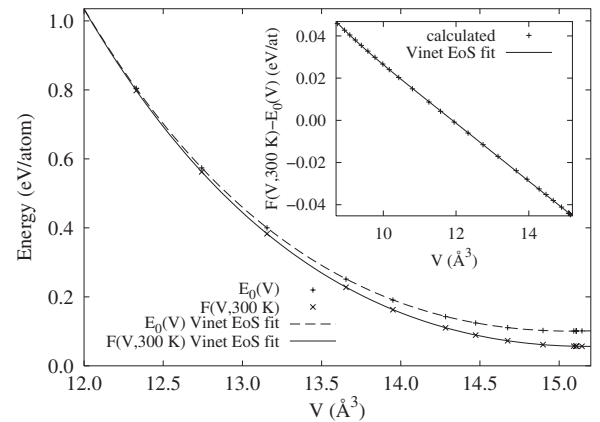
FIG. 2. Electronic energy and free energy vs volume for the stable fcc phase of Pt. Inset: the difference $F - E_0$; the symbols are calculated points, and the line is the difference of the Vinet EOSs of the main figure.

TABLE I. Values for the bulk modulus B_0, its pressure derivative B_0' and the equilibrium volume V_0 obtained from LDA calculation fitted with Vinet EOS.

Experiment at 300 K		
B_0 (GPa)	278[a]	271.5[b]
B_0'	5.61[a]	5.33[b]
V_{expt} (Å^3)	15.0948[c]	
Theory		
Pressure fitting range (GPa)	0–660	0–80
Volume fitting range (Å^3)	8.7–15.2	12.7–15.2
Fit to free energy at 300 K		
B_0 (GPa)	281	284
B_0'	5.61	5.57
V_0 (Å^3)	15.188	15.180
B_0 (V_{expt})	291	293
B_0' (V_{expt})	5.55	5.51
Fit to the electronic energy		
B_0 (GPa)	293	298
B_0'	5.56	5.46
V_0 (Å^3)	15.073	15.060
B_0 (V_{expt})	291	294
B_0' (V_{expt})	5.57	5.48

[a]Reference 5.
[b]Vinet fit of shock wave data of Ref. 6 in the range 0–80 GPa.
[c]Reference 25.

LDA equilibrium volume is smaller than the experimental one, as expected. The phonon contribution overcorrects the equilibrium volume. However, the difference between the highest and the lowest theoretical volumes is less than 1%, which is an excellent accuracy. The four fits provide similar bulk moduli and derivatives at the experimental unit cell volume. The bulk modulus at V_{expt} is 13–16 GPa higher than the measured values, which is a good agreement. All the fitted parameters in the present study are closer to the experimental values than those obtained in previous DFT calculations.

In the inset of Fig. 2, the points represent the calculated temperature correction $F(V,T) - E_0(V)$. The continuous line is not fitted to these data, but is the subtraction $F(V,T) - E_0(V)$ using the Vinet EOSs fitted independently to $F(V,T)$ and $E_0(V)$. The excellent agreement shows the ability of the Vinet EOS to fit not only the total energies, but also the differences simultaneously. Moreover, we have verified that the Vinet EOS is superior[27] to the Birch-Murnaghan EOS in the sense that the fitted values of the equilibrium volume, bulk modulus and its derivative are less dependent on the pressure range (see Table I).

The Vinet pressure-volume[24] (PV) EOS is given by

$$P = 3B_0 \frac{(1-X)}{X^2} e^{\eta(1-X)}. \tag{9}$$

We obtained the (PV) EOS using Eq. (9) with the parameters obtained by fitting Eq. (7). Figure 3 shows the PV diagram
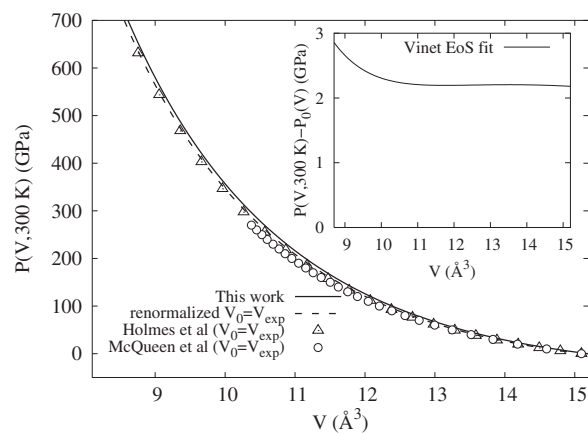
FIG. 3. Pressure vs volume for the stable fcc phase of Pt.

for $T=300$ K, together with the experimental data from Mc-Queen *et al.*[6] and the theoretical calculation of Holmes *et al.*[5] The inset of Fig. 3 shows the phonon contribution to the total pressure, i.e., the difference $\Delta P = -\partial F/\partial V + \partial E_0/\partial V$. It can be seen that our EOS agrees very well with the previous EOSs. Our pressures are slightly higher than those of Holmes *et al.*,[5] a fact also noticed and discussed in the recent report by Xiang *et al.*[7] We note that, at 270 GPa, the theoretical EOSs provide pressures that are 10–26 GPa in excess of the experimental pressure. The systematic appearance of this excess pressure suggests that this is the accuracy of the LDA for platinum. The frozen character of the $5s$ and $5p$ core states in the pseudopotential approximation may also contribute to the discrepancy. However, let us note that this discrepancy persists in the full-potential calculation of Xiang *et al.*, where the $5p$ states were treated as semicore states. When used as a standard in x-ray diffraction experiments, the pressure is computed using the measured relative volume V/V_0 in the platinum EOS. Hence, for a proper comparison with the Holmes *et al.* EOS, we renormalized our EOS to have $V_0 = V_{expt}$ and present it with a dashed line in Fig. 3. This improved the agreement between the theoretical EOSs. The pressures computed for a given set of V/V_0 using the present EOS and that of Holmes *et al.*[5] differ by an amount that increases from zero to less than 6 GPa in the pressure range 0–650 GPa. The pressures from the EOS of McQueen *et al.*[6] are lower than those computed from the present EOS. The difference reaches 16 GPa at 270 GPa, the highest pressure in the experiment.

From a fundamental point of view, it is interesting to plot the electronic and vibrational DOSs. Figure 4 shows the electronic density of states, the value of which at the Fermi level (taken as zero energy) gives the entropy contribution [Eq. (2)] to the free energy for selected volumes. Figure 5 displays the phonon density of states $g(\omega)$ for selected unit cell volumes.

III. ELASTIC CONSTANTS

The independent elastic stiffness constants in the cubic phase are C_{11}, C_{12}, and C_{44}. They were calculated at every pressure and zero temperature using the definition of the
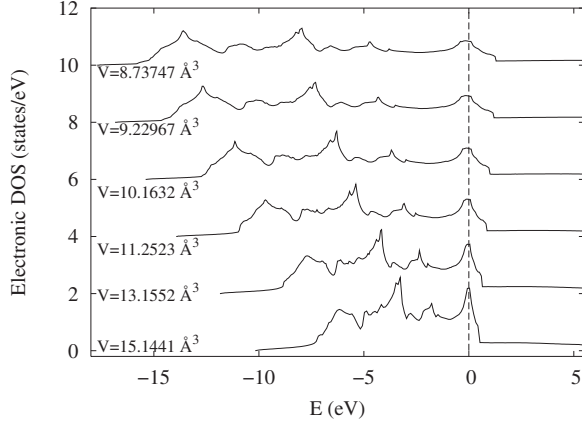
FIG. 4. Electronic density of states of Pt for different pressures.

stiffness constants in terms of the stress (σ_{ij}) and strain tensors (ε_{ij}),

$$C_{ijkl} = \frac{\partial \sigma_{ij}}{\partial \varepsilon_{kl}} \quad (i,j,k,l = x,y,z), \tag{10}$$

where we follow the usual convention $C_{11} = C_{xxxx}$, $C_{12} = C_{xxyy}$, and $C_{44} = C_{xyxy}$. For the constants C_{11} and C_{12} we deformed the unit cell as defined by the lattice vectors (in Cartesian coordinates)

$$\vec{a}_1 = a(0, 0.5, 0.5), \tag{11}$$

$$\vec{a}_2 = a(0.5 + 0.5\varepsilon_{xx}, 0, 0.5), \tag{12}$$

$$\vec{a}_3 = a(0.5 + 0.5\varepsilon_{xx}, 0.5, 0). \tag{13}$$

The derivative in Eq. (10) was evaluated numerically by making a series of calculations with $\varepsilon_{xx} = \{0.00, \pm 0.005, \pm 0.010, \pm 0.015\}$, and fitting the calculated σ_{xx} and σ_{yy} to a quadratic polynomial in ε_{xx}, the linear terms of which provide the elastic constants. The value of σ_{xx} at $\varepsilon_{xx} = 0$ provides the electronic pressure P_0, which is controlled through the lattice parameter a.

To obtain C_{44} we calculated σ_{xy} using the unit cell defined by the lattice vectors
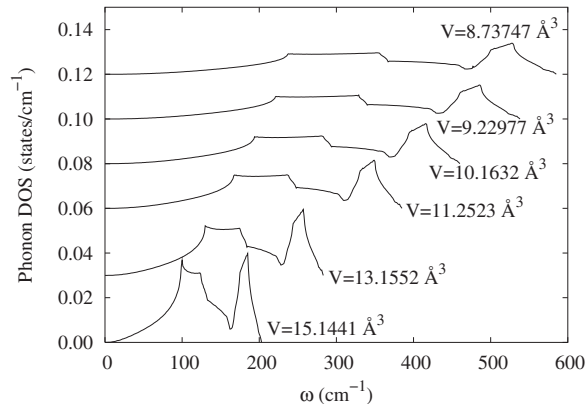
FIG. 5. Phonon density of states for different pressures.

TABLE II. Bulk modulus, elastic constants, and $S = 1/(C_{11} - C_{12}) - 1/2C_{44}$ of Pt at 300 K [from the $F(V,T)$]. P, B, and C_{ij} are in GPa, S is in GPa^{-1}. C_{44}(extpl) values obtained from the Birch extrapolation[14] formula with the experimental values $C_{44} = 73.243$ GPa and $C'_{44} = 1.6257$ from Ref. [17].

V (Å^3)	P	B	C_{11}[a]	C_{12}[a]	C_{44}[a]	C_{44}(extpl)	S
15.1075	1.4	295.9	359.4	264.1	74.9	74.9	0.0038
15.0650	2.2	300.4	364.7	268.2	76.4	76.3	0.0038
14.8984	5.6	318.4	386.2	284.4	82.5	81.4	0.0038
14.4729	15	369.8	446.6	331.4	100.1	96.9	0.0037
13.9505	30	444.0	533.1	399.4	125.5	118	0.0035
13.1552	60	583.6	695.4	527.7	175.4	158	0.0031
12.3300	104	774.5	915.7	703.9	238.8	212	0.0026
11.5730	160	1006	1180	918.3	318.2	276	0.0022
10.8004	239	1317	1534	1209	423.9	362	0.0019
10.1632	329	1653	1911	1524	535.7	453	0.0016
9.7709	399	1905	2192	1762	618.3	521	0.0015
9.3952	479	2186	2503	2028	703.7	597	0.0014
9.0765	559	2461	2804	2290	797.2	672	0.0013
8.7375	658	2796	3170	2610	902.1	763	0.0012

[a]We estimate that these values have only two significant figures. However, the extra figures in the C_{ij} are need to calculate the elastic compliances $S_{ij} = C_{ij}^{-1}$ and the S factor with similar precision.

$$\vec{a}_1 = a(\varepsilon_{xy}, 0.5, 0.5), \tag{14}$$

$$\vec{a}_2 = a(0.5, 0, 0.5), \tag{15}$$

$$\vec{a}_3 = a(0.5 + \varepsilon_{xy}, 0.5, 0). \tag{16}$$

The derivative in Eq. (10) was evaluated by the same procedure, using $\varepsilon_{xy} = \{0.00, \pm 0.005, \pm 0.010, \pm 0.015\}$.

For the calculation of the elastic constants, different from the EOS calculation, the electronic free energy and the stress tensor at 300 K were obtained directly from self-consistent calculations using the Fermi-Dirac smearing scheme, and a $45 \times 45 \times 45$ k-mesh. Phonon contributions and thermal corrections can be obtained from the second derivatives of the phonon free energy. At 300 K, the electronic free energy correction is negligible, and the phonon correction is smaller than the error of the calculation. Moreover, the S values calculated with this method exhibit noticeable scatter and do not show monotonic variation with pressure. This computational noise was mitigated, but not totally eliminated, using higher cutoffs, denser k meshes, and more fitting points to obtain the second derivatives of the free energy. Hence, we report in Table II only the elastic moduli calculated from the *ab initio* stresses without the phonon corrections. However, the pressure reported includes the phonon correction, which is important at low pressure.

IV. CONCLUSIONS

The equation of state of platinum to 650 GPa computed from first principles in this study is in excellent agreement

with that derived from shock-wave experiments and earlier first-principles calculations. Excellent agreement among the EOSs proposed by different investigators establishes platinum as a reliable pressure standard. A comparison of electronic energies indicates that the face-centered-cubic phase of platinum is more stable than the hexagonal-close-packed and body-centered-cubic phases to at least 650 GPa. This analysis considers truly hydrostatic pressure and does not rule out the possibility of some other phase being stabilized by shear stress, which is always present in experiments with diamond anvil cells. The computed single-crystal elastic constants at ambient pressure are in good agreement with those obtained from ultrasonic velocity measurements. The present calculations of C_{44} at high pressure agree well with the values derived from the Birch extrapolation formula with measured C_{44} and its pressure derivative at ambient pressure. The anisotropy parameter $(S_{11}-S_{12}-S_{44}/2)$ derived from the computed C_{ij} decreases with increasing pressure and stays positive in the 0–650 GPa pressure range.

[1] H. K. Mao, Y. Wu, L. C. Chen, J. F. Shu, and A. P. Jephcoat, J. Geophys. Res. **95**, 21737 (1990).

[2] D. Andrault, G. Fiquet, F. Guyot, and M. Hanfland, Science **282**, 720 (1998).

[3] Y. Akahama, H. Kawamura, and A. K. Singh, J. Appl. Phys. **92**, 5892 (2002).

[4] Y. Akahama, M. Nishimura, K. Kinoshita, H. Kawamura, and Y. Ohishi, Phys. Rev. Lett. **96**, 045505 (2006).

[5] N. C. Holmes, J. A. Moriarty, G. R. Gathers, and W. J. Nellis, J. Appl. Phys. **66**, 2962 (1989).

[6] R. G. McQueen, S. P. Marsh, J. W. Taylor, J. M. Fritz, and W. J. Carter, *High Velocity Impact Phenomena* (Academic, New York, 1970).

[7] S. Xiang, L. Cai, Y. Bi, F. Jing, and S. Wang, Phys. Rev. B **72**, 184102 (2005).

[8] F. D. Stacey and P. M. Davis, Phys. Earth Planet. Inter. **142**, 137 (2004).

[9] A. K. Singh, J. Appl. Phys. **73**, 4278 (1993).

[10] A. K. Singh, J. Appl. Phys. **74**, 5920 (1993).

[11] A. K. Singh, H.-K. Mao, J. Shu, and R. J. Hemley, Phys. Rev. Lett. **80**, 2157 (1998).

[12] A. K. Singh, C. Balasingh, H.-K. Mao, R. J. Hemley, and J. Shu, J. Appl. Phys. **83**, 7567 (1998).

[13] A. K. Singh, J. Phys. Chem. Solids **65**, 1589 (2004).

[14] F. Birch, J. Geophys. Res. **83**, 1257 (1978).

[15] S. M. Collard and McLellan, Acta Metall. Mater. **40**, 699 (1992).

[16] R. E. Macfarlane, J. A. Rayne, and C. K. Jones, Phys. Lett. **18**, 91 (1965).

[17] S. N. Biswas, M. J. P. Muringer, and C. A. ten Seldam, Phys. Status Solidi A **141**, 361 (1994).

[18] A. Kavner and T. S. Duffy, Phys. Rev. B **68**, 144101 (2003).

[19] S. Baroni, A. D. Corso, S. de Gironcoli, P. Giannozzi, C. Cavazzoni, G. Ballabio, S. Scandolo, G. Chiarotti, P. Focher, A. Pasquarello, K. Laasonen, A. Trave, R. Car, N. Marzari, and A. Kokalj, computer code QUANTUM ESPRESSO (2005), http://www.pwscf.org/

[20] M. Methfessel and A. T. Paxton, Phys. Rev. B **40**, 3616 (1989).

[21] O. H. Nielsen and R. M. Martin, Phys. Rev. Lett. **50**, 697 (1983).

[22] K. Laasonen, A. Pasquarello, R. Car, C. Lee, and D. Vanderbilt, Phys. Rev. B **47**, 10142 (1993).

[23] A. M. Rappe, K. M. Rabe, E. Kaxiras, and J. D. Joannopoulos, Phys. Rev. B **41**, 1227 (1990).

[24] P. Vinet, J. R. Smith, J. Ferrante, and J. H. Rose, Phys. Rev. B **35**, 1945 (1987).

[25] H. E. Swanson and E. Tatge, *Standard X-Ray Diffraction Powder Patterns*, Natl. Bur. Stand. (U.S.) Circ. No. 539 (U.S. GPO, Washington, D.C., 1953), Vol. I.

[26] R. E. Cohen, O. Gulseren, and R. J. Hemley, Am. Mineral. **85**, 338 (2000).

[27] Other arguments in favor of the Vinet EOS can be found in Ref. 26.